

Shear-Induced Transition of Originally Undisturbed Lamellar Phase to Vesicle Phase[†]

J. I. Escalante,[‡] M. Gradzielski,^{*,‡} H. Hoffmann,[‡] and K. Mortensen[§]

*Lehrstuhl für Physikalische Chemie I, Universität Bayreuth, D-95447 Bayreuth, Germany, and
Condensed Matter Physics and Chemistry Department, Risø National Laboratory,
DK-4000 Roskilde, Denmark*

Received February 18, 2000. In Final Form: July 11, 2000

We have studied the transformation of an L_α phase composed of stacked bilayers to a vesicle phase under the influence of shear. The ionically charged stacked bilayer phase was prepared by protonation of an L_3 phase from tetradecyldimethylamine oxide hexanol, and water. The protonation was accomplished by a hydrolysis reaction of an ester solubilized in this phase. By the protonation of the bilayers the L_3 phase becomes unstable and, in the absence of shear, is transformed into a classical lamellar phase. This low-viscosity phase was then transformed into an onion phase by shear. The structural changes during this transformation process were monitored by means of scattering experiments and by rheological and conductivity measurements under shear. The following results were obtained when the shear rate was varied: (a) the transition from stacked lamellae to vesicles is irreversible and does not go back; (b) the formation of multilamellar vesicles requires a total strain of about 2000 (for a given surfactant concentration of 100 mM). In addition the influence of various parameters on the transformations of the L_α phase was studied, such as chain length of the surfactant, chain length of the alcohol, and the total concentration of amphiphile.

Introduction

Many aqueous solutions of amphiphilic molecules are known to form lamellar liquid crystalline phases. For instance, such phases may be formed in mixtures of surfactants with n-alcohols. The lamellar phases can be stabilized by long-range repulsive interaction forces resulting from ionic charges or from thermal fluctuations of the membranes,¹ and for instance, they may be studied by light-scattering techniques.² Undulation forces dominate when the membranes are flexible, that is, in terms of the bending modulus: $\kappa \sim k_B T$, and electrostatic forces are absent or screened out.

In general shear flow can have a strong influence on the structure of complex fluids. Samples with lamellar morphology have especially attracted much attention in the past few years. In most experiments the stationary states that are reached for a constant shear rate have been investigated, but so far only little is understood about the kinetics of the structural transitions. Mang et al.³ have measured by small-angle X-ray scattering the behavior of a lamellar system under shear and found that the domains order in the direction of stress as the strain increases. Penfold et al.⁴ have investigated the alignment of lamellae under shear of aqueous hexaethylene glycol monohexadecyl ether ($C_{16}E_6$) samples in a Couette shear cell by small-angle neutron scattering experiments (SANS). They found that at low shear the lamellae are ordered parallel to the flow–vorticity plane. At intermediate shear rates a biaxial alignment has been found, whereas at high

shear rates the lamellae are oriented perpendicularly that is, parallel to the flow–shear gradient plane. These results agree with the theoretical predictions of Cates and Milner's theory.⁵

Roux and co-workers have come up with an orientation rheogram plotted on the $(\dot{\gamma}; \phi)$ plane, where $\dot{\gamma}$ is the shear rate and ϕ the volume fraction of bilayer membrane, which they assumed would be generally valid.⁶ Their results were obtained on a quaternary system of the anionic sodium dodecyl sulfate (SDS), pentanol, dodecane, and brine. It is shown for this system that a multidomain L_α phase is aligned by shear to a state in which the bilayers are oriented parallel to the wall of the Couette cell. At a threshold value of shear $\dot{\gamma}_c$ that is characteristic for the system, the bilayers break up and are transformed to vesicles. For $\dot{\gamma} > \dot{\gamma}_c$ a two-phase region exists in which extended bilayers are in equilibrium with vesicles. With increasing shear rate a single vesicle phase is reached that can exhibit a high degree of positional ordering.⁷ For even higher shear rates the vesicles are finally transformed to a perfectly aligned L_α phase that is supposed to be free of defects.

In some other studies the $L_\alpha \rightarrow$ vesicle transition was not observed. Instead, for a concentrated system of SDS/decanol it was shown that at intermediate shear rates the bilayers are aligned perpendicularly to the wall.⁸ At a second critical shear rate the bilayers are finally aligned parallel to the walls again. In our own investigations of charged L_α phases, the vesicle $\rightarrow L_\alpha$ transition was not observed at higher shear rates. Instead at the highest available shear rate of 6000 s^{-1} , unilamellar vesicles were formed.⁹ Finally, for the AOT system it was found that

* Author for correspondence.

[†] Part of the Special Issue "Colloid Science Matured, Four Colloid Scientists Turn 60 at the Millennium".

[‡] Universität Bayreuth.

[§] Risø National Laboratory.

(1) Helfrich, W. *J. Phys.: Condens. Matter* **1994**, 23, A 79.

(2) von Berlepsch, H.; Strey, R. *Colloid Polym. Sci.* **1994**, 272, 577.

(3) Mang, J. T.; Kumar, S.; Hammouda, B. *Europhys. Lett.* **1994**, 28, 489.

(4) Penfold, J.; Staples, E.; Khan Lodhi, A.; Tucker, I.; Tiddy, G. J. *T. J. Phys. Chem. B* **1997**, 101, 66.

(5) Cates, M.; Milner, S. F. *Phys. Rev. Lett.* **1989**, 62, 1865.

(6) Diat, O.; Roux, D.; Nallet, F. *J. Phys. II France* **1993**, 3, 1427.

(7) Diat, O.; Roux, D.; Nallet, F. *Phys. Rev. E: Stat. Phys., Plasmas, Fluids, Relat. Interdiscip. Top.* **1995**, 51, 3296.

(8) Berghausen, J.; Zipfel, J.; Lindner, P.; Richter, W. *Europhys. Lett.* **1998**, 43, 683.

(9) Bergmeier, M.; Gradzielski, M.; Hoffmann, H.; Mortensen, K. *J. Phys. Chem. B* **1999**, 103, 1605.

not the shear rate but the shear stress is the crucial parameter for the transformation, and here a perpendicular orientation was seen at high shear rates.¹⁰ In this paper it was also observed that the multilamellar vesicles (MLV) (onions) form an ordered state under shear.

In most of the investigations no detailed studies were made on the mechanism of the various phase transformations. In general it was observed that a stationary state for a given shear rate is reached only after fairly long times of several minutes to hours.¹¹ In a dynamic study of the transient behavior of the size changes of onions it has been seen that the size changes can occur in a continuous manner (for not too large differences between initial and final shear rates) or discontinuously (for large differences between initial and final shear rates).¹²

Considering the fact that quite different results were obtained for different surfactant systems, one can state that one is not yet in a position to have a general understanding of the shear-induced transformations that occur in lamellar amphiphilic systems. Therefore the aim of this work is to contribute to a more general understanding of the principles that govern the structural changes and in particular to study the kinetic aspects of these transformations. As mentioned above, this has not been done in much detail so far, although it can be expected that the dynamic aspects of these transformations are not only of interest by themselves but should be of principal importance regarding a systematic understanding of the morphological changes that take place.

A central point for such investigations is to start the shear experiments from a reproducible original state since we have observed before that the structure of a given system may depend sensitively on the shear history of a given sample, for example, an identical sample may contain MLV or stacked bilayers depending on whether it has been exposed to shear (like shaking) or not.¹³ To study this aspect in more detail we devised a strategy where one can pass from one well-defined phase to another well-defined phase by simple chemical reactions in which the whole system is at rest and no mixing and shearing of the systems is involved.¹⁴ The change of the micellar structures in the systems can be followed in situ by conductivity and rheological measurements¹⁵ or by scattering experiments and optical and electron microscopy.¹⁶

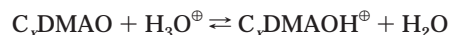
This concept of using a lamellar phase produced by a chemical reaction in a reproducible manner was applied by us for the systematic study of the effect that shear has on such samples. As system we chose a lamellar phase consisting of tetradecyldimethylamine oxide (C₁₄DMAO), hexanol, and water.¹⁷ As will be shown below, a well-defined L_α phase can be produced by protonation of an equilibrium L₃ phase. The L_α phase can then be transformed to MLV by shear where we investigated systematically the shear rate dependence of these transformations. Furthermore, in this system various parameters that control the stability of the L_α phase were varied. Such parameters are chain length of surfactant and cosurfac-

tants, or the total concentration of amphiphile. Once more it should be stressed that before its formation, the L_α state had not been exposed to shear. This procedure has the advantage over previous investigations in that the results do not depend on the history of preparation of the samples.^{13,14}

Experimental Section

Materials. All the chemicals used were obtained from commercial sources. The alkyl-dimethylamine oxides (C_xDMAO) were a gift from Clariant (Gendorf) and delivered as a 25% solution. They were recrystallized twice from acetone and characterized by the melting point and critical micelle concentration (cmc) before use [dodecyldimethylamine oxide (C₁₂-DMAO): mp 119–120 °C and cmc = 1.7 mmol/L; C₁₄DMAO: mp 130–131 °C and cmc = 0.14 mmol/L]. Diethyl oxalate (EO) (96% purity) was purchased from Merck, and the alcohols of p.a. purity (hexanol, heptanol, and octanol) were used without further purification and were purchased from Fluka. The water used in all experiments was doubly distilled and the D₂O (99.9% isotopic purity) used for the SANS experiments was obtained from Euriso-top, Groupe CEA, Saint Aubin (France).

Description of the System. C₁₂DMAO is soluble in water at room temperature (≈25 °C) and forms small micelles.¹⁸ C₁₄-DMAO forms spherical micelles above its cmc and rodlike micelles at higher concentrations.^{19–22} Hexadecyldimethylamine oxide (C₁₆DMAO) has a Krafft point around 28 °C.²³ The pK_a of monomeric C₁₂DMAO and C₁₄DMAO were found to be 4.95 and 4.9, respectively.¹⁹ In contrast to the normal nonionics with EO headgroups, the amine oxides have no cloud points, even in the presence of excess electrolyte. However, the amine oxides are coupled to an acid–base equilibrium:



and the phase diagram is affected by this equilibrium. The basicity of the oxide group is, however, rather weak, and only a few tenths of a percent of the compound are present in the protonated form when dissolved in water. C₁₄DMAOH⁺ and C₁₄DMAO show attractive interactions in micellar aggregates because of hydrogen bonding between the OH group of C_xDMAOH⁺ and the oxygen of C_xDMAO (where x = 12, 14, and 16).¹⁹ C₁₄DMAO forms vesicles in a three-component system containing C₁₄DMAO, *n*-hexanol, and water at certain compositions.²⁴ The degree of protonation of C₁₄DMAO in the micelles has an influence on the various phases and, therefore, on the formation of vesicles. Therefore the C₁₄-DMAO/*n*-hexanol/water system provides us with the opportunity to study phase transformations by changing the net charge of the aggregates by means of a chemical reaction.

Preparation of Samples. For the measurements, all the samples were prepared in the same way. First the optically isotropic, low viscosity L₃ phase was produced. The L₃ phase was then mixed with the appropriate amount of EO to obtain the desired charge density of the L_α phase. EO is soluble in the L₃ phase without destroying it (it has been shown before for the more slowly hydrolyzing methyl formate that it becomes incorporated into the L₃ phase without affecting its structure significantly¹³). Immediately after mixing, the sample was filled into the experimental device, for example, rheometer, Couette cell, etc. EO then hydrolyzes in the course of the next hour and the formed oxalic acid protonates the amine oxide. This causes the L₃ phase to be transformed to a classic multidomain L_α phase that consists of stacked bilayers. The L_α phase, when measured with oscillatory mode, is a low viscosity liquid that is very shear

(10) Bergenholtz, J.; Wagner, N. J. *Langmuir* **1996**, *12*, 3122.

(11) Shahidzadeh, N.; Bonn, D.; Aguerre-Chariol, O.; Meunier, J. *Phys. Rev. Lett.* **1998**, *81*, 4268.

(12) Panizza, P.; Colin, A.; Coulon, C.; Roux, D. *Eur. Phys. J. B* **1998**, *4*, 65.

(13) Hoffmann, H.; Bergmeier, M.; Gradzielski, M.; Thunig, C. *Prog. Colloid Polym. Sci.* **1998**, *109*, 13.

(14) Bergmeier, M.; Hoffmann, H.; Thunig, C. *J. Phys. Chem. B* **1997**, *101*, 5767.

(15) Escalante, J. I.; Hoffmann, H. *Rheol. Acta*, in press.

(16) Escalante, J. I.; Hoffmann, H. *Europhys. Lett.* (submitted for publication).

(17) Hoffmann, H.; Thunig, C.; Schmiedel, P.; Murkert, U. *Faraday Discuss.* **1995**, *101*, 319.

(18) Ikeda, S.; Tsunoda, M.; Maeda, H. *J. Colloid Interface Sci.* **1979**, *70*, 448.

(19) Rathman, J. F.; Christian, S. *Langmuir* **1990**, *6*, 391.

(20) Faucompre, B.; Lindman, B. *J. Phys. Chem.* **1987**, *91*, 383.

(21) Röhrig, H.; Stephan, R. In *Industrial Applications of Surfactants*; Karsa, D. R., Ed.; Cambridge, 1990.

(22) Hoffmann, H.; Oetter, G.; Schwandner, B. *Prog. Colloid Polym. Sci.* **1987**, *73*, 95.

(23) Oetter, G. Dissertation, Universität Bayreuth, 1989.

(24) (a) Hoffmann, H.; Thunig, C.; Munkert, U. *Langmuir* **1992**, *8*, 2629. (b) Simon, B. D.; Cates, M. E. *J. Phys. II* **1992**, *2*, 1439.

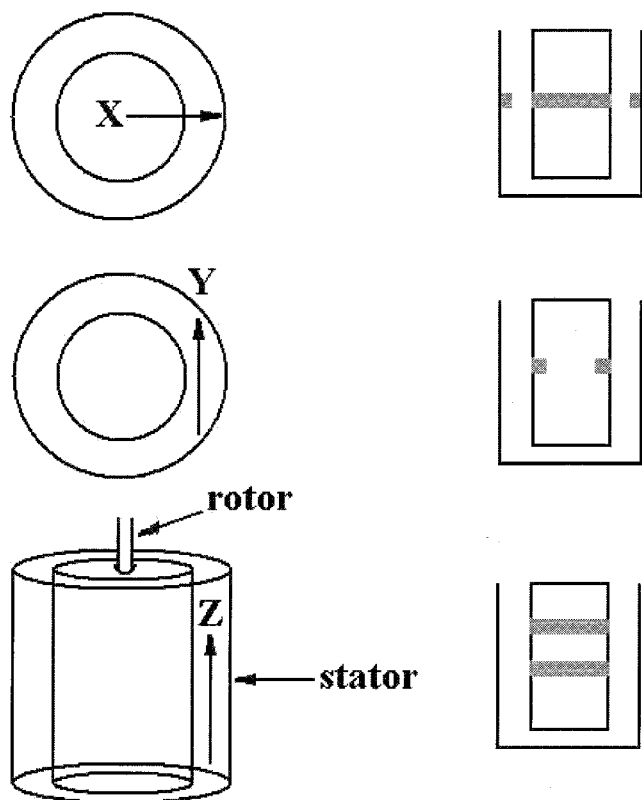


Figure 1. Sketch of a Couette cell as it was typically used in the experiments. Indicated are the x - (shear gradient), y - (flow), and z - (vorticity) directions.

sensitive. If instead the L_α phase is prepared by mixing oxalic acid with the L_3 phase, a strongly viscoelastic vesicle phase is obtained.²⁵

Methods. To measure the conductivity in the three main directions (shear gradient, velocity, and vorticity) we used a Couette cell described before⁹ and similar to the ones used to perform light, neutron, or X-ray scattering.²⁶ Depending on the position of the electrodes we have access to three different directions. Such a Couette cell is sketched in Figure 1 to show our definitions of x -, y -, and z -directions, which correspond to the direction of the shear gradient, the shear, and the vorticity, respectively. The electrical conductivity data were determined by means of a microprocessor conductivity meter, type Lf3000 (WTW, Weilheim, Germany), that measures the conductivity with a precision better than 0.5%. The apparatus was calibrated with a 10 mM KCl solution and the values for the cell constant were 0.016, 1.896, 0.925 cm^{-1} in x -, y -, and z -directions, respectively. All the measurements were done at 25 °C at constant shear rates in the range $1 \text{ s}^{-1} < \dot{\gamma}_c < 1000 \text{ s}^{-1}$.

The rheological measurements were carried out in a Bohlin CS 10 rheometer with a Couette geometry. The maximum permitted deviation in temperature was 0.1 °C during measurements. Before all measurements a sample of the L_3 phase was mixed with EO, stirred, and kept quiescently in the rheometer for 4 h. The apparent viscosity was measured by steady-state measurements. For the dynamical measurements (oscillation) we tested first the linear viscoelastic region. In all the cases we observed that there is reproducibility of the data.

Neutron scattering experiments were performed with the instrument SANS at the Risø National Laboratory in Roskilde, Denmark. The scattering data were collected on a 128*128 2-D detector and corrected for background and empty cell scattering. A wavelength of 4.7 Å and a sample-to-detector distance of 6 m were used, thereby covering a range of momentum transfer q from 9×10^{-3} to $6.5 \times 10^{-2} \text{ Å}^{-1}$. The Couette-type shear cell has a gap of 1 mm. In the standard configuration called the radial-

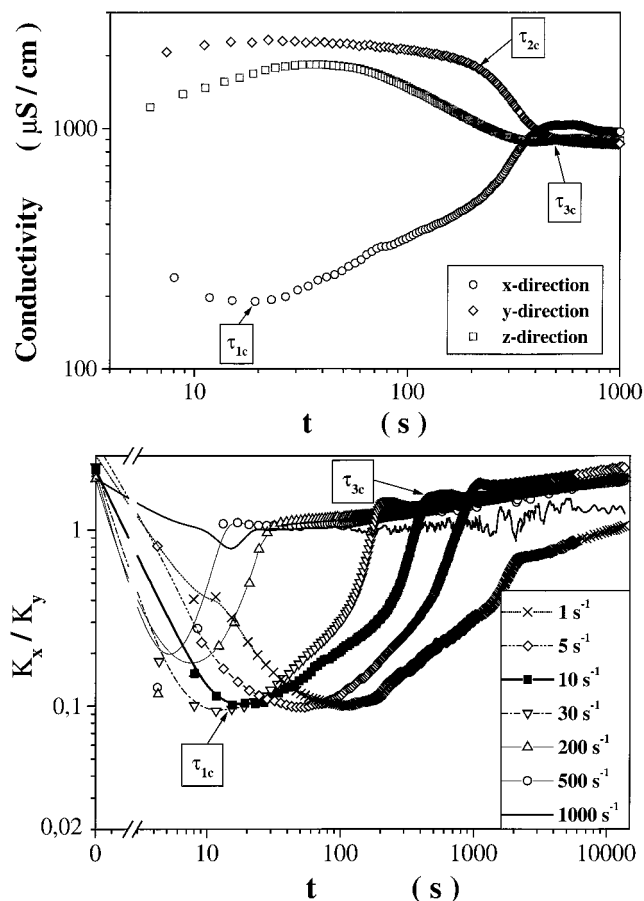


Figure 2. (Top) Electrical conductivities in x -, y -, and z -directions as a function of time for a sample of 100 mM C_{14} -DMAO/10 mM EO/250 mM hexanol/water (after termination of the hydrolysis reaction) when a shear rate of 10 s^{-1} was applied (shear was turned on at $t = 0$; $T = 25 \text{ °C}$). (Bottom) The ratio of the conductivities in the direction of the shear gradient and the flow, K_x/K_y , as a function of time for various shear rates.

beam geometry the incident beam is aligned parallel to the shear gradient. A detailed description of the shear cell has been given elsewhere.²⁷

For the freeze-fracture transmission electron microscopy (FF-TEM), a small amount of the sample was placed on a 0.1-mm-thick copper disk and covered with a second copper disk. The probe was frozen by plunging it into liquid propane, which was cooled by liquid nitrogen. Fracturing and replication were carried out in a BALZERS BASF 400 FF apparatus at a temperature of -140 °C. Pt/C was deposited under an angle of 45°. The replicas were examined in a CEM 902 electron microscope (Zeiss, Germany).

Results and Discussion

Shear-Induced Transitions in the System 100 mM C_{14} -DMAO/10 mM EO/250 mM 1-Hexanol/Water. Conductivity Data. Conductivity measurements in a Couette cell in all three different directions were made as a function of shear rate, and continuous changes of the conductivities K_x , K_y , K_z with time were recorded (Figure 2 top). The L_α phase at rest has a high conductivity because the bilayers are mainly oriented arbitrarily and the charged species can pass from one electrode to the other without having to cross the bilayers. On the other hand, when an L_1 phase from C_{14} -DMAO (and without cosurfactant) was mixed with oxalic acid, the resulting phase had a much higher

(25) Bergmeier, M.; Gradzielski, M.; Thunig, C.; Hoffmann, H. *Nuovo Cimento* **1998**, *20D*, 2251.

(26) Vinches, C.; Coulon, C.; Roux, D. *J. Phys. II* **1994**, *4*, 1165.

(27) Nordén, B.; Elvingson, C.; Eriksson, T.; Kubista, M.; Sjöberg, B.; Takahashi, M.; Mortensen, K. *J. Mol. Biol.* **1990**, *216*, 223.

conductivity for the same charge density value (by a factor of 2.6). In the L_1 phase the ions can move in a direct route from one electrode to the other without having to take detours as in the L_α phase.

Under shear the largest changes were found in the x -direction (κ_x), that is, the direction of the shear gradient (Figure 2, top). First κ_x decreases rapidly until it reaches a minimum. Then it increases continuously again until at large times a plateau value is reached. κ_y and κ_z both increase somewhat with time, reach a maximum, and then decrease again until after long times a plateau value is reached that is almost identical for all three directions.

In Figure 2 (top) clearly three distinct characteristic times can be ascribed to the description of the transformation process of the lamellar phase. The first time τ_{1c} is the time to reach the minimum in κ_x (which typically is on a similar time scale as the maxima of κ_y and κ_z which, however, are less pronounced). The second time τ_{2c} is the time after which a break of the conductivity in flow direction, κ_y , is observed. The third time τ_{3c} then is the time all three conductivities level off to reach a plateau value.

To have a more precise measure, one can make a comparison between the conductivities of the L_α phase with the L_1 phase in both directions, parallel and perpendicular to the director. Thus one obtains a value for the anisotropy of the conductivity, given by

$$\frac{K_x}{K_y} = \frac{K_{x_{L_\alpha}}/K_{x_{L_1}}}{K_{y_{L_\alpha}}/K_{y_{L_1}}} = A \quad (1)$$

where $K_{x_{L_\alpha}}$ and $K_{y_{L_\alpha}}$ are the conductivity measurements of the lamellar phase in shear and flow direction, respectively, and $K_{x_{L_1}}$ and $K_{y_{L_1}}$ are the conductivity values of the L_1 phase.

One can study quantitatively the process of alignment of the lamellae and their transformation to vesicles by using this relation for the anisotropy of the conductivity (eq 1). The value of K_x/K_y is a quantitative measure for the orientation of the bilayers where parallel orientation of the bilayers should lead to values much smaller than 1 and perpendicular orientation to values around 1. For the case of vesicles that are deformed by the shear field, values smaller than 1 are also to be expected (depending on the degree of deformation of the vesicles in the shear field). From Figure 2 (bottom) it is clear that the alignment of the lamellae is a function of the time and shear rate in such a way that the transformations occur the faster and higher the applied shear rate. Before shear is applied, the conductivity is about the same in both directions because the multidomain lamellar phase in the system is not aligned (here the precise values of the conductivity are mainly determined by the history of the filling process).

For example, for the case of a shear gradient of 10 s^{-1} , K_x/K_y decreases rapidly after turning on the shear, and at its minimum (τ_{1c}) it is about 10 times lower than for the solution at rest. After the minimum at about 20 s the conductivity anisotropy in the double log plot increases more or less linearly with time until it reaches at τ_{3c} some sort of a plateau value (where, however, still some slower increase of K_x/K_y can be observed).

The first minimum corresponds to the situation where the bilayers are best aligned parallel to the wall. At larger times the degree of parallel orientation of the bilayers decreases. This could be explained by a flip of the lamellae into a perpendicular orientation or alternatively by an equilibrium between vesicles and bilayers that is shifted in favor of the vesicles with increasing time. However,

Table 1: Ratio of Conductivities in Shear Gradient and Flow Direction in the Long Time Limit and Time Constants τ_1 , τ_2 , and τ_3 as Obtained from the Rheological (r) and Electrical Conductivity (c) Measurements for Different Shear Rates for a System of 100 mM C_{14} DMAO/10 mM EO/250 mM 1-Hexanol/Water

$\dot{\gamma}/\text{s}^{-1}$	K_x/K_y	τ_{1c}/s	τ_{2c}/s	τ_{3c}/s	τ_{3r}/s	τ_{3c}/s
1	1.07	108	1510	2450	5290	3400
3	1.08	82	660	710	1940	1220
5	2.32	44	240	420	810	790
10	2.42	24	230	300	640	440
30	1.95	14	68	122	222	210
200	1.93	<4	-	22	-	41
500	1.86	<4	-	9	-	14
1000	1.36	<4	-	-	-	12

looking at Figure 2 (top) there is clear indication that there occurs first a flip into perpendicular orientation before the formation of vesicles. This can be inferred from the fact that κ_z decreases much earlier than κ_y . For the case of vesicle formation both should be affected similarly. In addition, one finds that the conductivity in the vorticity direction, κ_z , is always significantly smaller than that in the flow direction, κ_y , which is a further indication for a perpendicular orientation of the lamellae. Therefore the logical conclusion is that for the case depicted in Figure 2 (top) the flip into perpendicular orientation occurs after about 30 s, whereas vesicle formation only starts after about 200 s, as indicated by the decrease of κ_y (τ_{2c}). This means that before vesicle formation, already a reorientation of the originally parallel-oriented bilayers to a perpendicular orientation has taken place.

At the break point (τ_{3c} , defined by the intersection of the linearized decrease of κ_y with the plateau region after the break), this transformation to vesicles is basically over and the further small increase of K_x/K_y could be due to rearrangements in the size distribution of the vesicles. The results for the time constants are summarized in Table 1 together with the long time limiting value for K_x/K_y . It is interesting to note that this value for K_x/K_y is always larger than 1. The value first increases with increasing shear rate, whereas at high shear rates the observed anisotropy decreases again. This decrease could be explained by the fact that at such high shear rates the vesicles become increasingly deformed.

At this point it is noteworthy to stress again that the conductivity data indicate a state in which the bilayers are aligned perpendicularly to the wall. Such a stationary orientation has been proposed by several groups on the basis of SANS data.²⁸ However, in our case this state is observed at intermediate times (deformations) before the formation of vesicles.

For all cases the conductivity data in the x -direction are similarly related to the conductivity data in z - and y -directions. The minimum for the x -direction corresponds to a maximum in the z and y -directions. For a comparison the conductivity data for the y -direction are shown in Figure 3. Here the conductivity data were plotted versus the deformation, $\dot{\gamma}\tau$, and one finds that in general the data follow exactly the same trend that even with only minor adjustments can be folded on to a single master curve. The shift of the curves in Figure 3 to larger values of the deformation $\dot{\gamma}\tau$ with increasing shear rates could be due to the fact that the transformation from planar lamellae to vesicles will take place most effectively at low shear rates. With increasing shear rate an increasing amount of the energy that is required for the transforma-

(28) Weigel, R.; Lauser, J.; Richtering, W.; Lindner P. *J. Phys. II* **1996**, *6*, 529.

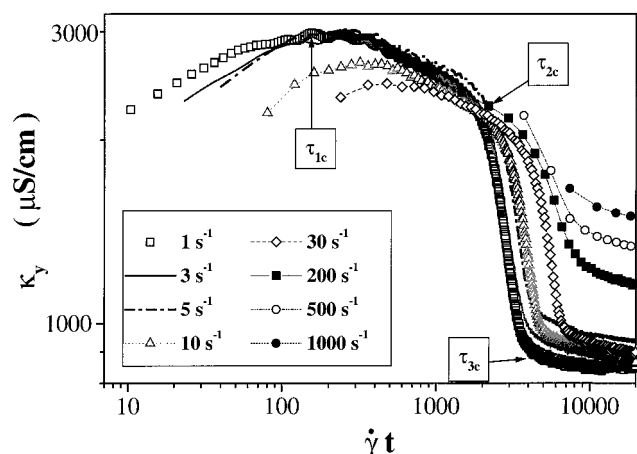


Figure 3. Electrical conductivity in flow direction (κ_y) as a function of the deformation for the system 100 mM C_{14} DMAO/10 mM EO/250 mM hexanol/water for various constant shear rates.

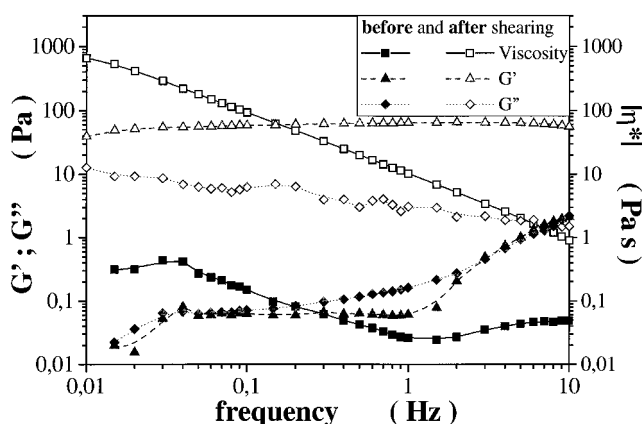


Figure 4. Rheogram of the sample 100 mM C_{14} DMAO/10 mM EO/250 mM hexanol/water (after termination of the hydrolysis reaction) at 25 °C, before and after a shear rate of 10 s⁻¹ had been applied for 2 h.

tion to vesicles will be dissipated by other mechanisms. Even more important is the fact that the final state of the vesicles depends on the shear rate applied, since we have shown before that in the systems studied the final size of the vesicles formed decreases with increasing shear rate.⁹ This effect is most pronounced for the high shear rates and explains why here significant deviations have to be expected (the formation of more and smaller vesicles evidently requires more energy). However, our data actually demonstrate clearly that within a certain range of shear rates the phases pass through exactly the same structural state with time.

Rheological Results. The viscosity of the sample was monitored throughout the transformation process in all cases. Figure 4 is a dynamical rheogram for the unsheared low-viscosity L_α phase and for the MLV phase that was obtained from the L_α -phase by applying a constant shear rate of 10 s⁻¹ for 2 h. The unsheared L_α phase is weakly viscoelastic, with a viscosity of 40 mPa s. In contrast, the MLV phase is strongly viscoelastic, with a constant storage modulus (G') of about 60–70 Pa, which is about 1 order of magnitude larger than the loss modulus (G''). Such a behavior is typical for the systems with MLV, which are highly viscoelastic, behave like a Bingham fluid, and have a yield stress value.

In Figure 5 the time-dependent apparent viscosity is shown for an L_α phase exposed to a constant shear rate of 10 s⁻¹. For other shear rates similar curves were

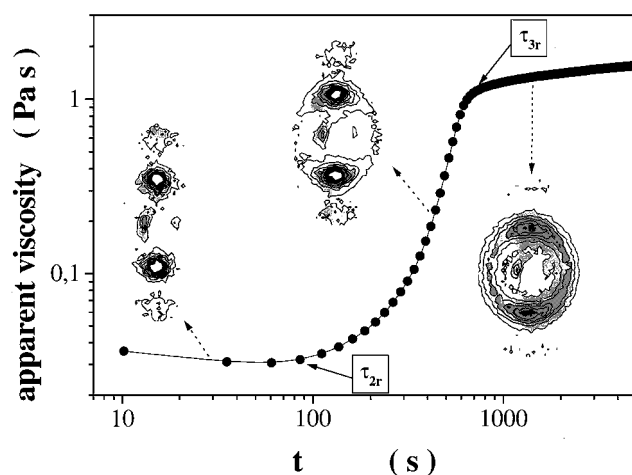


Figure 5. Apparent viscosity of the sample 100 mM C_{14} DMAO/10 mM diethyl oxalate/250 mM hexanol/water (after termination of the hydrolysis reaction) as a function of time after applying a constant shear rate of 10 s⁻¹. Inside are some corresponding curves from the SANS measurements.

Table 2: Time Constants τ_1 , τ_2 , and τ_3 as Obtained from Rheological (r) and Electrical Conductivity (c) Measurements for Surfactants of Different Alkyl Chain Length and a Composition of 100 mM C_x DMAO/10 mM EO/(240, 250, 245 for $x = 12, 14, 16$, respectively) mM Hexanol/Water (shear rate: 10 s⁻¹)

surfactant	τ_{1c}/s	τ_{2r}/s	τ_{2c}/s	τ_{3r}/s	τ_{3c}/s
C_{12} DMAO	24	90	150	500	300
C_{14} DMAO	20	140	200	700	420
C_{16} DMAO	30	190	230	800	400–700

obtained. At short times the viscosity decreases somewhat with time and then abruptly increases until it reaches a plateau value with some slight further increase of viscosity with time. With increasing shear rate the curves are shifted to shorter times.

To analyze the curves in a more quantitative way, two time constants can be assigned to this graph: the time constant τ_{2r} , which is the time to reach the minimum in the viscosity, and the time constant τ_{3r} , which is the time to reach the plateau value (precisely, we defined τ_{3r} by the intersection of the linearized increase of viscosity and the linearized plateau region of curves such as Figure 5). By comparing these time constants measured at different $\dot{\gamma}$, one finds that the product of τ and $\dot{\gamma}$ is constant ($\dot{\gamma} \cdot \tau_{2r} \approx 2000$, $\dot{\gamma} \cdot \tau_{3r} \approx 5000$, see Table 1). It is interesting to note that we never reached a completely stationary state even for very long times. The time constant τ_{2r} may be associated with the time to align the multidomain L_α phase and transfer a certain portion of the lamellae into the perpendicular orientation. The driving force for such an orientational flip could be to minimize the resistance of the system to shear (it might be noted that τ_{2r} is about a factor of 10 larger than τ_{1c} of the conductivity measurements). However, evidently here around τ_{2r} the formation of vesicles sets in, which is responsible for the following large increase of viscosity. τ_{2r} always has a similar but somewhat smaller value as τ_{2c} (cf. also Figure 3 and Tables 1–4), which is reasonable as the real onset of the viscosity increase (which really indicates the vesicle formation and should for that matter better be compared to τ_{2c}) occurs at somewhat larger times. Finally, τ_{3r} is the time constant (as defined by reaching the plateau value of the viscosity) associated with the formation of MLV and corresponds well to the values τ_{3c} derived from conductivity measurements (see Table 1).

Table 3: Time Constants τ_1 , τ_2 , and τ_3 as Obtained from Rheological (r) and Electrical Conductivity (c) Measurements for Surfactants of Different Alkyl Chain Length and a Composition of 100 mM C₁₄DMAO/10 mM EO/250 (185,160) mM Hexanol (Heptanol, Octanol)/Water (shear rate: 10 s⁻¹)

cosurfactant	τ_{1c}/s	τ_{2r}/s	τ_{2c}/s	τ_{3r}/s	τ_{3c}/s
hexanol	20	100	150	600	480
heptanol	45	120	410	1200	850
octanol	50	140	400	1500	1000

Table 4: Time Constants τ_1 , τ_2 , and τ_3 as Obtained from Rheological (r) and Electrical Conductivity (c) Measurements for Samples of the Given Composition that Always Contained 10 mol % (with Respect to Surfactant) of EO (shear rate: 10 s⁻¹)

C ₁₄ DMAO/hexanol	τ_{1c}/s	τ_{2r}/s	τ_{2c}/s	τ_{3r}/s	τ_{3c}/s
50/170	22	60	90	560	420
100/250	20	100	150	600	480
150/350	32	110	180	900	780
200/450	32	100	175	-	1000
300/745	45	120	205	-	620

Figure 5 also includes contour plots of SANS obtained under identical shear conditions, which reveal additional information about the structural changes that take place during shear. The flow direction (y) is horizontal in the contour plots, and the vorticity direction (z) vertical. The scattering pattern at short times is characterized by two pronounced peaks in the vorticity direction. In the region of increasing viscosity the two peaks are still present but become less and less pronounced, as would be expected for the case of vesicle formation. At long times the scattering pattern is only somewhat anisotropic, but still the correlation peak is well visible, a behavior that would be expected for the presence of MLV (which are deformed because of the presence of the shear field). In general, the scattering patterns observed support strongly the notion of having perpendicular orientation of bilayers before the formation of vesicles, as has already been inferred from the conductivity data.

Figure 6 clearly demonstrates the irreversibility of the changes occurring. It should be noted here that the time for increase/decrease of the viscosity was chosen to be 20 min, that is, one is in the limit of only applying the given shear rate for a relatively short time. As we have seen above, the process is largely governed by the deformation applied, and it increases progressively along the x -axis of Figure 6. One can see three regimes, first the shear thinning (at low shear rates) where the sample behaves like a plastic fluid, such as the L_{ah} phase with extensive bilayers. We can say that this thinning is principally due to the formation of ordered bilayer structures being aligned in the flow direction.^{29,30} In the second region a shear thickening is observed when $\dot{\gamma}$ exceeds a critical shear rate $\dot{\gamma}_c$ ($\dot{\gamma}_c \approx 10$ s⁻¹). This could be explained by the fact that at this point some of the bilayers start to close, resulting in the formation of vesicles that are more viscous than extended bilayers. Upon further increase of the shear rate one observes a maximum, which means that here most of the bilayers form closed structures (MLV) and behave in the same way as the L_{al} phase, a highly viscoelastic phase. The vesicles in these samples already have to be packed very densely. The third regime is characterized by another shear thinning. This is produced

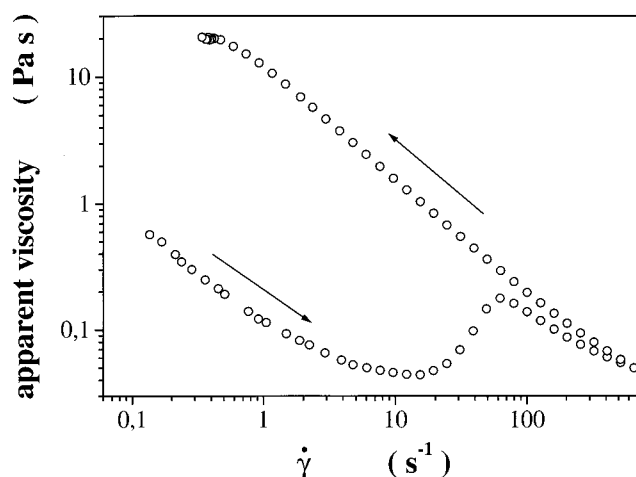


Figure 6. Apparent viscosity of the sample 100 mM C₁₄DMAO/10 mM EO/250 mM hexanol/water (after termination of the hydrolysis reaction) as a function of the shear rate. The total time for the increase/decrease of the shear rate was chosen to be 20 min for each direction.

by the alignment of new MLV during shearing, or once the vesicles are large enough they start to be deformed or ruptured.

However, upon reducing the shear rate again one observes no reversibility for the viscosity values, but instead one finds significantly larger values of the viscosity on reducing the shear rate in comparison with the ones observed when increasing the shear rate. This is due to the fact that the vesicles formed are long-time stable and the viscosity of the vesicle phase is about 2 orders of magnitude larger than that of the corresponding lamellar phase of stacked bilayers.

FF-TEM. The TEM images were prepared from samples that contained about 20% glycerol. The glycerol was added to suppress the formation of ice crystals during the freezing process. Figure 7 shows TEM images of the system 100 mM C₁₄DMAO/10 mM diethyl oxalate/250 mM hexanol/water at room temperature: (a) FF electron micrograph of the L_α phase after the hydrolysis reaction; (b) micrograph of the MLV obtained by application of a shear rate of 1 s⁻¹ for about 1 h in a steady-state measurement.

Clearly visible is that the system before the application of shear contains stacked lamellae that exhibit relatively strong undulations. The micrograph for the sheared sample looks completely different. Here no extended lamellae are visible, but all of the surfactant appears to be transformed into vesicles. The vesicles are very polydisperse in size ranging from small unilamellar vesicles of 40 nm diameter to MLV (onions) of more than 1 μ m diameter.

SANS. To complement the above experiments with further structural data, SANS experiments were performed under similar rheological conditions. The objective was to obtain a more detailed picture of the shear-induced lamellae to vesicle transformation.

The starting L₃ phase was prepared as described before (for the SANS experiments D₂O was used instead of H₂O, but this had practically no influence on the phase behavior of the systems under study). The progress of the ester hydrolysis was monitored continuously by SANS measurements. After about 2 h the samples were subjected to a constant shear gradient of 10 s⁻¹.

Figure 8 shows the azimuthally obtained averaged SANS curves for the L_α phase as a function of the time after turning on a shear rate of 1 s⁻¹. At $q \approx 0.015$ Å⁻¹ for all cases a characteristic peak and its second order at

(29) Laun, H. M.; Bung, R.; Hess, S.; Loose W.; Hess, O.; Hank, K.; Hädicke, E.; Hingmann, R.; Schmidt, F.; Lindner, P. *J. Rheol.* **1992**, *36*, 743.

(30) Montalvo, G.; Rodenas, E.; Valiente, M. *J. Colloid Interface Sci.* **1998**, *202*, 232.

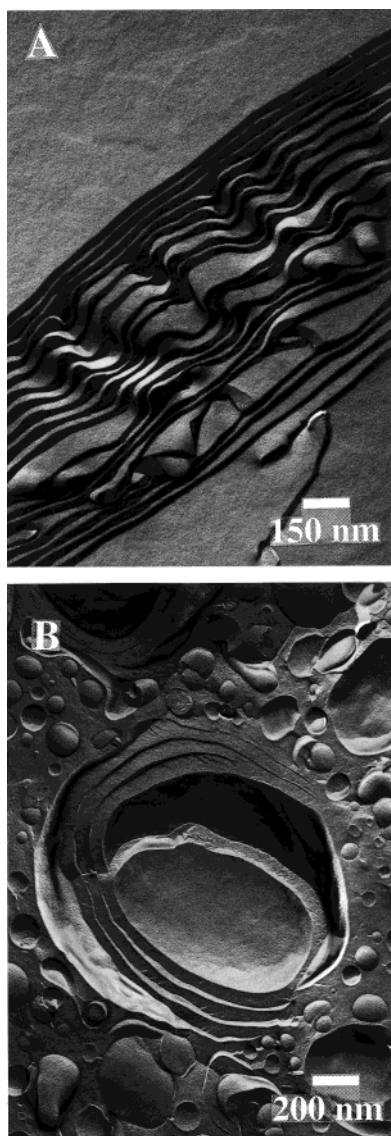


Figure 7. FF-TEM micrographs that were prepared from a sample of 100 mM C_{14} DMAO/250 mM hexanol/water that was mixed with 10 mM EO and contained 20% glycerol in the water. (A) Sample after 1 h of hydrolysis; (B) same sample having been exposed to a shear rate of 10 s^{-1} for 1 h.

twice the q value are observed, from which the mean distance d of the bilayers can be determined to be about 450 Å. In general the azimuthally averaged scattering curves change only little in appearance. The q -value for the peak position increases somewhat with increasing time, which means that the mean bilayer spacing becomes somewhat larger. Such a behavior is in agreement with a formation of vesicles because in the vesicles the bilayers are less effectively packed.

As a simple measure of the anisotropy we defined an anisotropy factor $A = I_z/I_y$. The values of I_z/I_y as a function of time for the system 100 mM C_{14} DMAO/250 mM hexanol/ D_2O are shown in Figure 9. From this graph we can assign the different arrangements of the lamellae as well as their transformation to vesicles. At short times one observes an overshoot of I_z/I_y , which indicates a high degree of order of the lamellar phase. A significant decrease of the anisotropy occurs exactly at the same time when in Figure 2 (top) κ_y starts to decrease. The long time limit of the anisotropy A is not equal to 1, but A levels off around $A = 1.8$, which is quite similar to the value observed in for κ_x/κ_y in the conductivity (cf. Table 1).

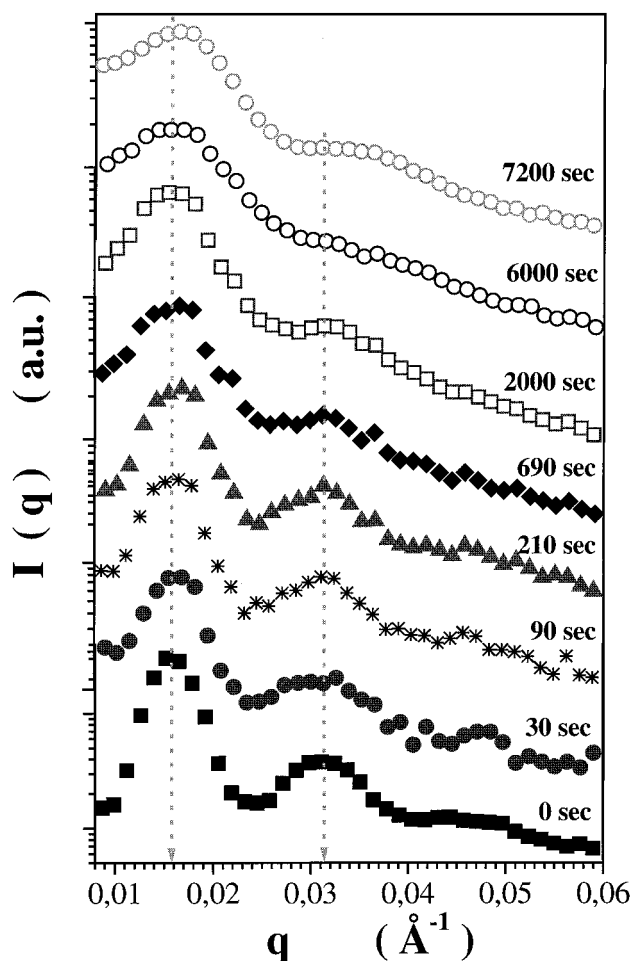


Figure 8. Azimuthally averaged SANS curves of the system 100 mM C_{14} DMAO/10 mM EO/250 mM hexanol/ D_2O (after termination of the hydrolysis reaction) for various times after a shear rate of 10 s^{-1} was applied. The data obtained from the initial L_α phase (before shear) are represented by closed squares.

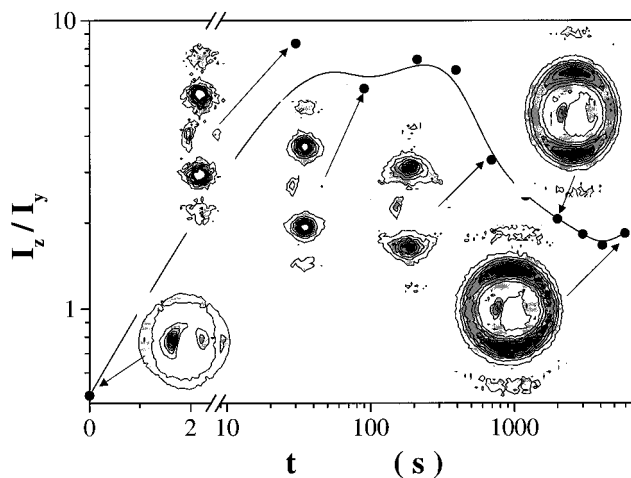


Figure 9. Anisotropy factor A ($A = I_z/I_y$) of the SANS measurements for the system 100 mM C_{14} DMAO/250 mM hexanol/10 mM EO/ D_2O as a function of time for a constant shear rate of 10 s^{-1} . Inside are some of the contour plots of the corresponding SANS patterns.

Figure 9 also includes some of the corresponding contour plots of the SANS patterns. The first pattern corresponds to the L_α phase formed at the end of the hydrolysis reaction and before shear. One can see two pronounced peaks in horizontal direction since because of the filling process,

the director of the lamellae is preferentially oriented in the plane perpendicular to the vorticity direction.

The second pattern was measured around 40 s after application of a shear rate of 10 s^{-1} . It is characterized by two peaks perpendicular to the flow direction. This indicates a change of the arrangement of the lamellae to a perpendicular orientation (although it should be noted here that a parallel orientation is not visible in radial geometry chosen for the experiment). The orientation even increases somewhat with elapsing time (third pattern). This point corresponds to the τ_2 zone in the conductivity and rheology experiments. This point of largest anisotropy we can associate with the onset of the transition from lamellae to vesicle, that is, after this point the perpendicularly oriented lamellae start to break and form vesicles, which should lead to a decrease of the high anisotropy.

At longer times the degree of orientation diminishes clearly (fourth pattern), and patterns 5 and 6 (which belong to times somewhat larger than τ_{3c}) are already characterized by a scattering ring with only a fairly small degree of anisotropy due to the shear deformation of the vesicles. According to the rheological and conductivity measurements vesicles should be present here, and the scattering pattern confirms this assumption because the pattern looks exactly as would be expected for MLV with a similar interlamellar spacing as the previously present lamellar phase.

Influence of Chain Length of the Surfactant. To generalize the above findings we studied the influence of the alkyl chain length of the surfactant on the properties of the L_α phase under shear (again obtained from the hydrolysis of an L_3 phase). The surfactants used for these investigations were dodecyl-, tetradecyl-, and hexadecyldimethylamine oxide ($C_x\text{DMAO}$; $x = 12, 14$, and 16). The L_3 phase was in all the cases produced with 1-hexanol as cosurfactant and for constant surfactant concentration of 100 mM (with 240, 250, 245 mM 1-hexanol for $x = 12, 14, 16$, respectively).

The apparent viscosity as a function of time (Figure 10 top) always changes similarly, and mainly a shift to lower values with increasing chain length is found. In addition, one observes some increase of the characteristic times (τ_{2r} and τ_{3r}) with increasing chain length of the surfactant. Compared with $C_{14}\text{DMAO}$, τ_{2r} and τ_{3r} for $C_{12}\text{DMAO}$ are approximately halved. In the case of the $C_{16}\text{DMAO}$ the change is less clearly pronounced, but one observes that even after more than half an hour the viscosity was still increasing markedly. It is interesting to note that the final viscosity is higher the shorter the chain length of the surfactant.

Figure 10 (bottom) shows the ratio of the conductivities κ_x/κ_y for different alkyl chain lengths of the surfactant. The same behavior is observed as in the rheological measurements. But here the increase of the characteristic times with increasing chain length is more evident. One also observes that the minimum associated with τ_{1c} becomes much less pronounced with decreasing chain length (in particular for going from $C_{14}\text{DMAO}$ to $C_{12}\text{DMAO}$). On the basis of these results we may conclude that the transformation from lamellae to vesicles occurs faster with shorter chain length of surfactant. The results for the characteristic times obtained from rheological and conductivity data are summarized in Table 2.

Influence of Chain Length of Alcohol. As a further extension of our investigation, the influence of the chain length of the alcohol (cosurfactant) in the system 100 mM $C_{14}\text{DMAO}/C_y\text{OH}$ (where $y = 6, 7$, and 8 ; hexanol, heptanol, and octanol) was studied. Again, always such an amount

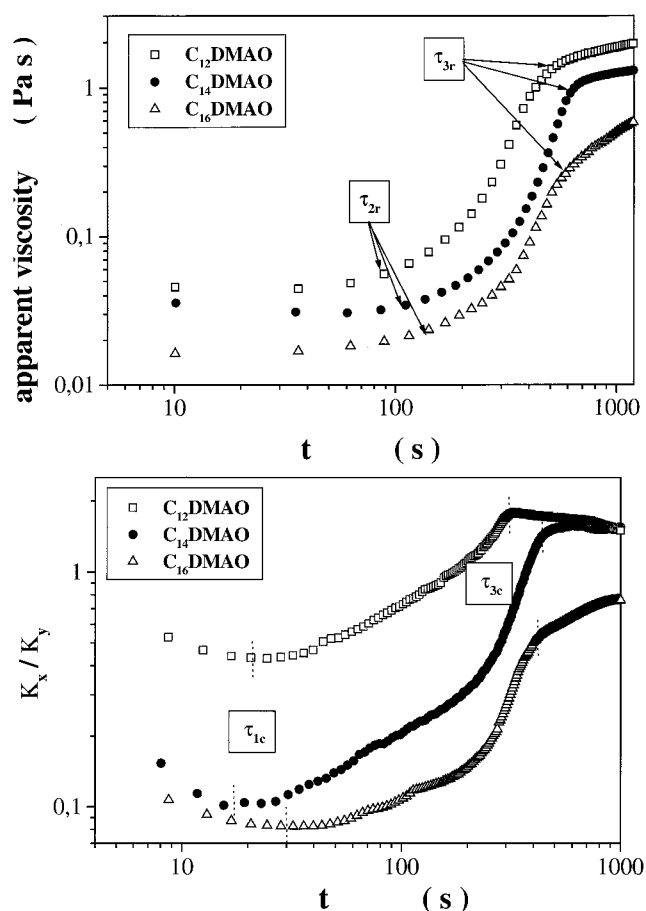


Figure 10. (Top) Apparent viscosity of the sample 100mM $C_x\text{DMAO}/250 \text{ mM}$ hexanol/10 mM EO/water (where $x = 12, 14$, and 16) as a function of time after application of a constant shear rate of 10 s^{-1} . (Bottom) Ratio of the conductivities recorded in the shear gradient (x) and flow (y) directions of the sample 100 mM $C_n\text{DMAO}/10 \text{ mM}$ EO/250 mM hexanol/water (where $n = 12, 14$, and 16) (after termination of the hydrolysis reaction) as a function of time after application of a constant shear rate of 10 s^{-1} .

of alcohol (250, 185, 160 mM for hexanol, heptanol, octanol, respectively)³¹ was added that one had the L_3 phase as a starting phase.

In Figure 11 (top) rheological data are shown for the produced lamellar phases with the different alcohols for the case of applying a constant shear rate of 10 s^{-1} . For heptanol and octanol the viscosity shows an overshoot before reaching a plateau value that becomes more pronounced with increasing chain length of the alcohol (and is absent for hexanol). This overshoot occurs in the τ_3 region, where mainly vesicles should be present. The origin of the overshoot is not clear at the moment. It is also interesting to note that the final apparent viscosity reached is about a factor of 4 higher for hexanol than for the longer-chain alcohols heptanol and octanol, which show almost identical values. However, it is evident from Figure 11 (top) that the characteristic time constants for the transformation become larger with increasing chain length of the alcohol.

The conductivity data (Figure 11, middle) also show that the transformation becomes slower with increasing chain length of the cosurfactant. Quite pronounced is the increase of the time required to achieve parallel orientation of the lamellae (τ_{1c}). Evidently it becomes more difficult

(31) Miller, C. A.; Gradzielski, M.; Hoffmann, H.; Krämer, U.; Thunig, C. *Prog. Colloid Polym. Sci.* **1991**, *84*, 243.

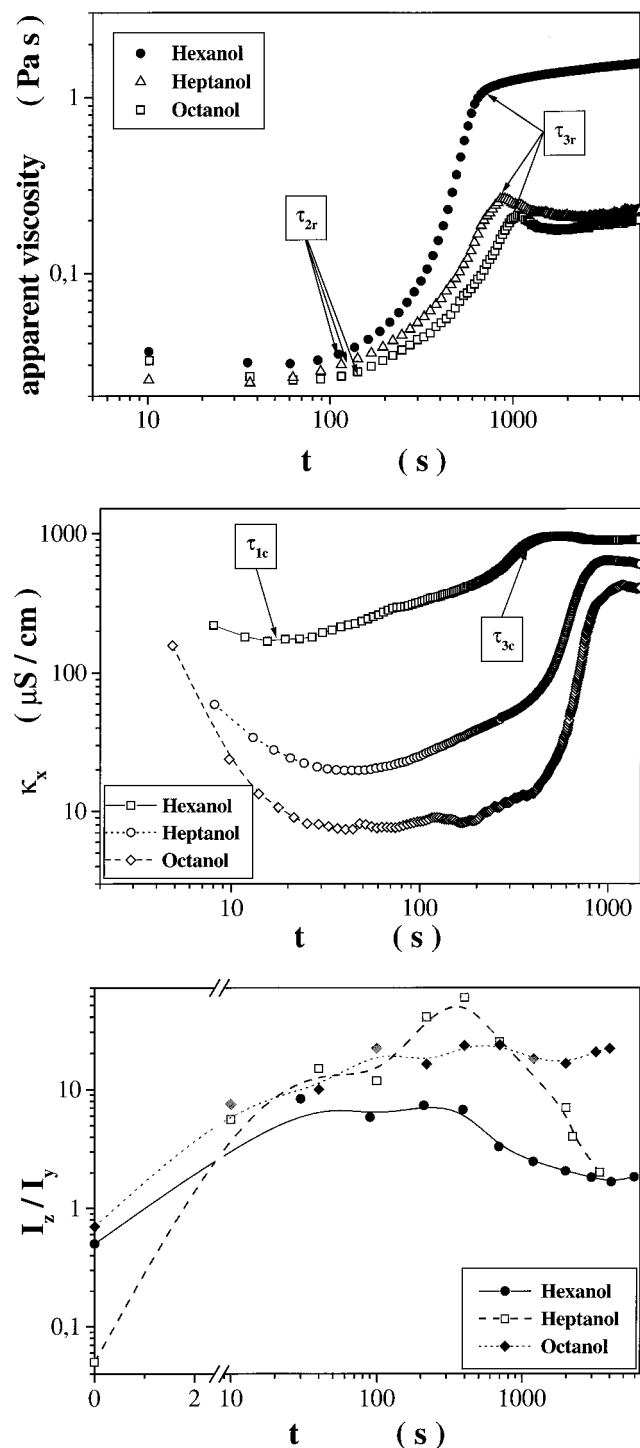


Figure 11. (Top) Apparent viscosity of the sample 100 mM $\text{C}_{14}\text{DMAO}/10 \text{ mM EO}/n \text{ mM C}_y\text{OH}/\text{water}$ (where $y = 6, 7$, and 8 and $n = 250, 185$, and 160 , respectively) (after termination of the hydrolysis reaction) as a function of time after application of a constant shear rate of 10 s^{-1} . (Middle) Electrical conductivity recorded in the direction of the shear gradient (x) of the sample 100 mM $\text{C}_{14}\text{DMAO}/10 \text{ mM EO}/n \text{ mM C}_y\text{OH}/\text{water}$ (where $y = 6, 7$, and 8 and $n = 250, 185$, and 160 , respectively) (after termination of the hydrolysis reaction) as a function of time after application of a constant shear rate of 10 s^{-1} . (Bottom) Anisotropy ratio I_z/I_y of the SANS measurement for the system 100 mM $\text{C}_{14}\text{DMAO}/10 \text{ mM EO}/n \text{ mM C}_y\text{OH}/\text{water}$ (where $y = 6, 7$, and 8 and $n = 250, 185$, and 160 , respectively) (after termination of the hydrolysis reaction) as a function of the time after application of a constant shear rate of 10 s^{-1} .

to orient the lamellae of the longer cosurfactants, which could be explained by the fact that at the same time the

thickness of the lamellae increases with increasing chain length of the cosurfactant.⁹ Thicker lamellae should be stiffer and therefore offer more resistance to reorientation. In addition, it should be noted that the degree of orientation or the number of defects in x -direction increases largely by increasing the chain length of the alcohol (as evidenced by the pronouncedness of the minimum of κ_x). The time constants τ_{2c} and τ_{3c} that are related to the formation of MLV are similarly affected and increase by about a factor of 2.

A comparison of the anisotropy factor I_z/I_y derived from the SANS experiment (Figure 11 bottom) shows the same trend of increasing time required for the transformations with increasing chain length of the alcohol. Also, the degree of perpendicular orientation increases with increasing chain length of the alcohol. From the high value of I_z/I_y after more than an hour for octanol it appears that even after this long time the transformation from lamellae to vesicle is not yet complete. We observed that only for a deformation approximately 10 times larger than the largest used shown here was the transformation for this sample complete.

Influence of Total Concentration of the Amphiphile. We also investigated the influence of the total concentration of amphiphilic material on the transition from the lamellar phase to the vesicle phase. To always start from an L_3 phase, different ratios of $\text{C}_{14}\text{DMAO}/\text{hexanol}$ had to be used for this investigation (Table 4). In general this is a more complex variation of the system than before because here one changes the interactions between the different lamellae significantly.

Figure 12 (top) shows the apparent viscosity obtained for the different concentrations of the L_α phase obtained from the protonation reaction of their respective L_3 phases (with an amount of added EO that corresponded to 10 mol % with respect to the surfactant). All measurements were done at 25°C and with a shear gradient of 10 s^{-1} . No large general difference is found for the different concentrations, that is, the characteristic times are similar and increase somewhat with increasing concentration (cf. Table 4). The final apparent viscosity increases with increasing total concentration. It should be noted that the samples with high surfactant concentration (200 and 300 mM C_{14}DMAO) do not reach a plateau value. This is due to the fact that these samples were very viscous and the shear stress reached the experimental limits.

The conductivity data in flow direction (Figure 12, middle) show an increase of τ_{1c} with increasing total concentration, that is, evidently the parallel alignment of the lamellae takes longer in the more concentrated systems, an effect that one might expect. Also, the time constant τ_{3c} increases correspondingly (Table 4), which means that their transformation to vesicles also becomes slower. The conductivity decreases with increasing concentration, which at first sight might be surprising because the concentration of counterions increases parallel to the surfactant concentration. However, the decrease may be explained by the fact that the more concentrated samples form MLV with an increasing number of shells and therefore trap an increasing percentage of the counterions. In addition, one can expect the system to be more densely packed, which will also render the electric conductivity lower simply by obstruction effects.

Finally, SANS experiments were carried out for the 100, 200, and 300 mM C_{14}DMAO samples. The change of the anisotropy factor I_z/I_y as a function of time (Figure 12 bottom) confirmed that the time required for the transformation to take place increases with increasing concentration. It is interesting to note that for the most

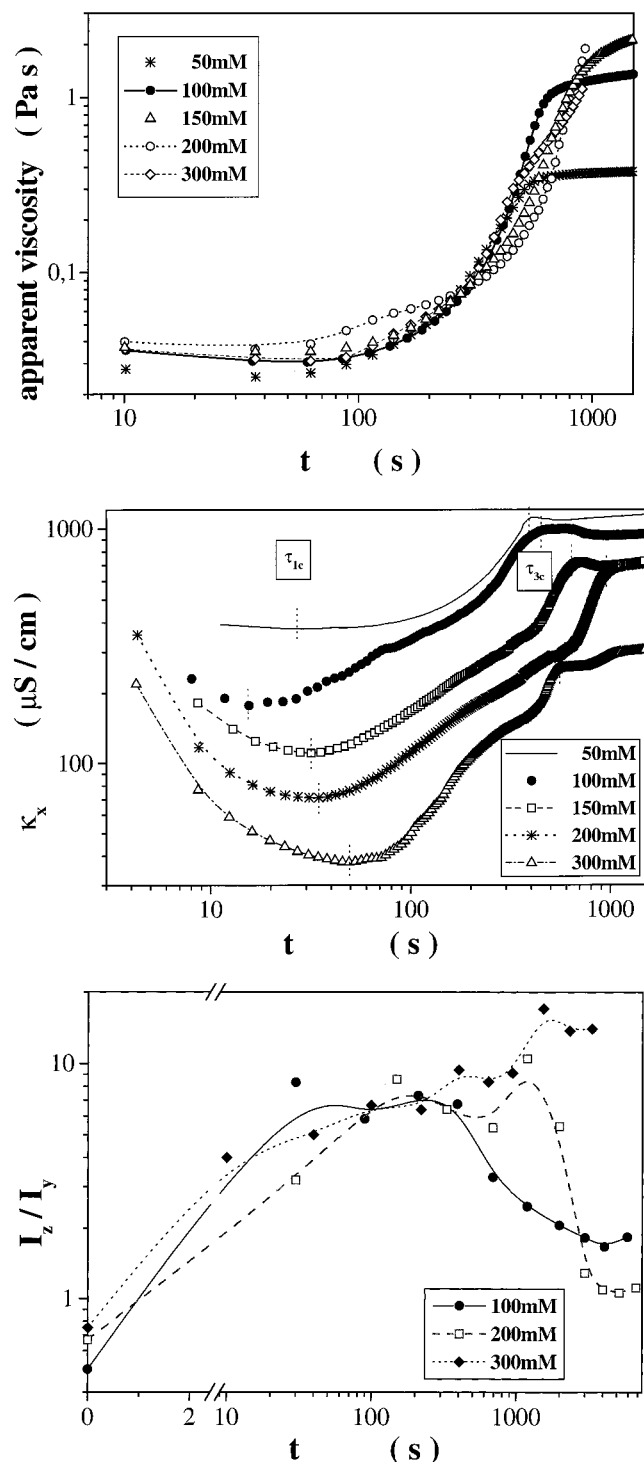


Figure 12. (Top) Apparent viscosity for samples of C_{14} DMAO, EO, hexanol, and water (after termination of the hydrolysis reaction) of various total concentrations as a function of time after application of a constant shear rate of 10 s^{-1} . (Middle) Electrical conductivity in direction of the shear gradient (x) for samples of C_{14} DMAO, EO, hexanol, and water (after termination of the hydrolysis reaction) of various total concentrations as a function of time after application of a constant shear rate of 10 s^{-1} . (Bottom) Anisotropy ratio I_z/I_y of the SANS measurement for the system C_{14} DMAO, EO, hexanol, and water (after termination of the hydrolysis reaction) of various total concentrations as a function of time after application of a constant shear rate of 10 s^{-1} .

concentrated sample (300 mM) the anisotropy is still very high, even for times longer than an hour, whereas it decreases to a value somewhat larger than 1 for the less

concentrated samples. This may be an indication that in the case of the 300 mM sample, indeed no vesicles are formed but that here still lamellar structures remain present, a tendency that has been observed before in similar systems.³² This would also explain why in the conductivity experiments the 300 mM sample shows a somewhat deviating behavior with respect to the fact that here τ_{3c} does not increase any more with increasing concentration (cf. Table 4 or Figure 12 middle).

Conclusions

The effect of shear on a lamellar phase composed of the zwitterionic surfactant C_x DMAO (that became charged by 20 mol % through a protonation reaction) and a medium-chain alcohol as cosurfactant has been investigated. The advantage of this lamellar phase over previously used lamellar phases is that it could be prepared in situ, that is, one circumvents the problem of a prior shear history for these samples. This is a very important point because evidently such phases are very sensitive to shear and results obtained otherwise can largely be influenced by the method of preparation of the lamellar phase.

The shear induced changes were studied by means of FF-TEM, and rheological, conductivity, and SANS measurements, and these experiments showed that the application of shear always leads to a transformation of the lamellar phase to MLV.

From the experiments, three characteristic times have been assigned to the transformation process (this can be done most clearly from the conductivity measurements but also from the rheological and SANS experiments, and the times obtained are in good agreement). The shortest time (only seen in the conductivity measurements) can be associated with the orientation parallel to the wall of the originally present lamellae in the shear field. The second time is the onset of the transformation of lamellae to vesicles and corresponds to a decrease of conductivity in flow direction and a minimum in the apparent viscosity. The third time is the one required to complete the conversion of planar lamellae to multilamellar vesicles and corresponds to reaching constant values for conductivity and viscosity. For a given system these characteristic times depend strongly on the shear rate used. Our experiments demonstrated that the relevant physical quantity in that context is the deformation applied to the system, that is, the characteristic times are inversely proportional to the shear rates used.

A very interesting point that could be observed by means of the SANS experiments (and is corroborated by the conductivity data) is that for all cases investigated one always observes a perpendicular orientation of the lamellae before the formation of vesicles. Apparently such an orientation is required before vesicle formation takes place, and starting from the perpendicular orientation the vesicles begin to be formed in the shear field once a characteristic deformation has been applied to the system. However, it is unclear at the moment why a fairly large deformation of typically ≈ 2000 is required before the formation process of the vesicles starts.

To generalize our findings we studied similar systems where the chain length of the surfactant, the chain length of the cosurfactant, and the total concentration of amphiphilic material were varied. These experiments showed that the characteristic times required for the transformations to take place increase both with increasing chain length of the surfactant and increasing chain length of

(32) Bergmeier, M. Dissertation, Universität Bayreuth, 1998.

the cosurfactant. However, in both cases the thickness of the bilayers also increases and evidently the thicker bilayers offer more resistance to the shear-induced transitions.

Similarly, we found that the transformation process requires more time with increasing concentration. This appears to be reasonable because one may imagine that the transformation of planar bilayers to closed vesicles requires a certain amount of energy per bilayer area. This energy has to be supplied by the shear process and, of course, more energy (and therefore more time for a given shear rate) will be required per given volume for more concentrated systems.

In summary, we can state that the process of formation of MLV in our system occurs via well-defined intermediate structures (like a perpendicular orientation of the bilayers before vesicle formation). It takes place in a very similar fashion for a large variety of different systems and over a large range of shear rates used. For a given system the characteristic parameter for the transformation process is the deformation applied. This means that one can produce such vesicle systems in a very well controlled

manner and obtain systems of desired properties by accordingly adjusting the composition of the starting system and choosing the corresponding shear conditions. Such a well-controlled formation of vesicle systems can be of importance for a variety of applications in cosmetics, pharmacy, food processing, etc. where such vesicles of well-defined properties are often required.

Acknowledgment. We are grateful to the German Ministry for Education and Research (BMBF) for financial support of this project and the Risø National Laboratory for financial support of the SANS experiments, through the large installation program of the European Community. We would also like to thank K. Horbaschek for the preparation of the electron micrographs, and W. Ulbricht and S. Schmölder for help with the SANS experiments. J.I.E. is grateful to the DAAD, CONACyT, and the University of Guadalajara (PROMEP's program) for financial support. Finally, we are indebted to H. R. Brand and G. K. Auernhammer for instructive discussions.

LA000242C